J Biomol NMR (2009) 44:167–173
DOI 10.1007/s10858-009-9326-y

COMMUNICATION

Selective backbone labeling of proteins using {1,2-$^{13}C_2$}-pyruvate as carbon source

Chenyun Guo · Chun Geng · Vitali Tugarinov

Received: 27 March 2009 / Accepted: 11 May 2009 / Published online: 26 May 2009

Abstract A simple isotope labeling approach for selective $^{13}C/^{15}N$ backbone labeling of proteins is described. Using {1,2-$^{13}C_2$}-pyruvate as the sole carbon source in bacterial growth media, selective incorporation of $^{13}C^{\alpha}$-^{13}CO spin-pairs into the backbones of protein molecules with medium-to-high levels of ^{13}C-enrichment is possible for a subset of 12 amino acids. The isotope labeling scheme has been tested on a pair of proteins—a 7-kDa immunoglobulin binding domain B1 of streptococcal protein G and an 82-kDa enzyme malate synthase G. A number of protein NMR applications are expected to benefit from the {1,2-$^{13}C_2$}-pyruvate based protein production.

Keywords Selective isotope labeling · {1,2-$^{13}C_2$}-Pyruvate · Protein backbone · MSG

Abbreviations

MSG	Malate synthase G
GB1	Immunoglobulin binding domain B1 of streptococcal protein G
HSQC	Heteronuclear single-quantum coherence
TROSY	Transverse relaxation optimized spectroscopy
3-PG	3-Phosphoglycerate
TCA	Tricarboxylic acid cycle
PEP	Phosphoenolpyruvate
OA	Oxaloacetate
AKG	α-Ketoglutarate
R5P	Ribose-5-phosphate
TPP	Thiamine pyrophosphate

C. Guo · C. Geng · V. Tugarinov (✉)
Department of Chemistry and Biochemistry, University of Maryland, College Park, MD 20742, USA
e-mail: vitali@umd.edu

The labeling of proteins with stable $^{13}C/^{15}N/^{2}H$ isotopes has been at the cornerstone of a variety of biomolecular NMR applications in the past two decades (Kainosho 1997; Goto and Kay 2000; Lian and Middleton 2001; Kainosho et al. 2006; Tugarinov et al. 2006). The types of NMR experiments that can be performed on a protein sample are oftentimes predicated upon the isotope labeling strategy chosen for sample production. Among the vast array of developed isotope labeling strategies for NMR studies of biomolecules, the labeling techniques that allow selective incorporation of isotopic labels into a (small) subset of nuclei in proteins play a special role. For example, producing deuterated proteins with selective $^{13}C/^{1}H$ labeling at specific methyl positions has been widely instrumental in the studies of high-molecular-weight proteins (Rosen et al. 1996; Gardner et al. 1997; Gardner and Kay 1998; Tugarinov et al. 2004, 2006). Selective rather than uniform incorporation of ^{13}C into backbone and side-chain positions of proteins usually pursues the goal of eliminating undesired ^{13}C-^{13}C scalar and dipolar couplings between directly bonded ^{13}C spins. The recent upsurge of interest in selective rather than uniform incorporation of ^{13}C nuclei into polypeptide chains of small-to-medium sized proteins led to a 'revival' of several old as well as the development of a number of new protocols for protein over-expression in minimal media using a variety of selectively labeled carbon sources. {1,3-$^{13}C_2$}- and {2-^{13}C}-glycerol were used earlier by (LeMaster and Kushlan 1996) as the primary carbon sources for incorporation of ^{13}C with alternating ^{13}C-^{12}C labeling patterns for ^{13}C relaxation studies. Recently, Wagner and co-workers have used a similar labeling strategy in conjunction with deuteration for direct $^{13}C^{\alpha}$ detection in fast-relaxing protein systems (Takeuchi et al. 2008). The same group has recently proposed selective ^{13}CO labeling on a deuterated background for NMR

studies of large proteins (Takeuchi et al. 2007). {1-^{13}C}- and {2-^{13}C}-glucose used as carbon sources have been shown to lead to selective ^{13}C incorporation in aromatic/methyl positions (Teilum et al. 2006; Lundström et al. 2007) and backbone C^{α} sites (Lundström et al. 2007), respectively.

The use of selectively ^{13}C-labeled pyruvate as the main carbon source in bacterial growth media has certain advantages over selectively ^{13}C-labeled glucose-based protein production. For example, in the process of glycolysis, two molecules of pyruvate are generated from {1-^{13}C}- and {2-^{13}C}-glucose—one with the desired labeling pattern that is later incorporated into amino-acids of the polypeptide chain, and the other unlabeled—thus effectively reducing the labeling efficiency to a maximum of 50% (Lundström et al. 2007). Clearly, pyruvate-based production avoids such a dilution of isotopic labels at the outset of amino-acid biosynthesis. Selective ^{13}C enrichment of Valγ, Leuδ, Ileγ2, Alaβ, and Metε methyl positions in proteins for methyl-directed relaxation studies can be achieved by the use of {3-^{13}C}-pyruvate-based media (Lee et al. 1997; Ishima et al. 2001). Recently, selective ^{13}C labeling at backbone carbonyl positions has been achieved by Kay and co-workers in {1-^{13}C}-pyruvate-based medium doped with ^{13}C-sodium carbonate ($NaH^{13}CO_3$) for ^{13}CO-directed relaxation dispersion measurements (Lundström et al. 2008; Hansen et al. 2008). Here, we complement all these approaches by a brief description of how selective backbone labeling of proteins can be achieved by growing bacterial cells in either H_2O- or D_2O-based minimal media with {1,2-$^{13}C_2$}-labeled pyruvate as the sole carbon source. The use of $^{15}NH_4Cl$ as nitrogen source leads to uniform and complete ^{15}N labeling of all nitrogen positions in the protein, whereas the $^{13}C^{\alpha}$-^{13}CO pairs of nuclei are generated in the protein backbone with varying degrees of incorporation efficiency. Selective incorporation of $^{13}C^{\alpha}$-^{13}CO spin-pairs into protein backbones with medium-to-high levels of ^{13}C-enrichment is possible for a subset of 12 amino acids.

Following the analysis of amino-acid biosynthetic pathways described by Lundström et al. (2007, 2008) in a couple of recent publications, we concentrate on *simultaneous* ^{13}C incorporation into C^{α} and CO positions of different amino-acids in {1,2-$^{13}C_2$}-pyruvate-derived proteins. In conjunction with uniform ^{15}N labeling, isolated $^{13}C^{\alpha}$-^{13}CO spin pairs would allow magnetization transfer along the protein backbone for a variety of NMR applications. Figure 1a shows a schematic pathway of amino-acid biosynthesis when {1,2-$^{13}C_2$}-labeled pyruvate is used as the sole carbon source. Based on their metabolic precursors all amino acids can be grouped into the following three categories (Takeuchi et al. 2008):

I Ala, Lys, Val originating directly from pyruvate; Cys, Gly, Ser, Trp originating from 3-phosphoglycerate (3PG); Phe and Tyr derived from phosphoenolpyruvate (PEP);
II Asn, Asp, Ile, Met, and Thr derived from oxaloacetate (OA);
III Glu, Gln, Arg, Pro originating from α-ketoglutarate (AKG).

The amino-acids of group I are expected to be $^{13}C^{\alpha}$-^{13}CO labeled at the level of close to 100% (if auxiliary biosynthetic pathways in *E. coli* are neglected), except Lys that can also be synthesized from OA (Fig. 1a). The amino-acids derived from OA (group II) are simultaneously labeled at both C^{α} and CO positions only before the molecules of OA enter the first TCA cycle; after the first (and subsequent) passes through the TCA cycle, ^{13}C enrichment would be restricted to either C^{α} or CO positions (considering that the molecules of succinate and fumarate are symmetric, after the first passage through the TCA cycle OA can be ^{13}C-enriched equiprobably at positions 1,3 and 2,4; Fig. 1a). Finally, the amino acids originating from AKG (group III) are not expected to obtain simultaneous $^{13}C^{\alpha}$-^{13}CO enrichment. Analysis of ^{13}C enrichment patterns attainable after further (up to the fourth) passes through the TCA cycle (not shown in Fig. 1a) leads to the conclusion that neither OA- (group II) nor AKG- (group III) derived amino acids are expected to be ^{13}C-enriched at both C^{α} and CO sites simultaneously.

The scheme of Fig. 1 predicts that the generation of $^{13}C^{\alpha}$-^{13}CO pairs in the pyruvate- and OA-derived groups (I and II) will be selective in the sense that C^{β} side-chain positions will not be ^{13}C-enriched in all these amino-acids except Val and Ile. Figure 1b shows the metabolic pathways for Val, Ile biosynthesis illustrating that the ^{13}C label is indeed expected to be retained at both C^{α} and C^{β} positions of these residues. The biosynthetic pathway of Leu (Fig. 1c) branches off from the valine pathway at α-ketoisovalerate. Leu C^{α} positions derived from the unlabeled methyl group of acetyl-CoA, are therefore not expected to be ^{13}C-enriched. Finally, histidines are synthesized from ribose-5-phosphate (R5P) via the pentose phosphate pathway with ^{13}C enrichment at R5P positions 1 through 4. Therefore, His C^{α} sites (derived from position 4 of R5P) will be ^{13}C-labeled, whereas carbonyls of His (derived from position 5 of R5P) will remain ^{12}C.

The {1,2-$^{13}C_2$}-pyruvate-based labeling scheme has been tested on a 7-kDa immunoglobulin binding domain B1 of streptococcal protein G (GB1) and an 82-kDa malate synthase G (MSG). Although the labeling strategy described here is likely to be applicable to small and medium-sized proteins, we have chosen to use the abundance of amino-acid content in the 723-residue MSG (Tugarinov et al. 2002) to

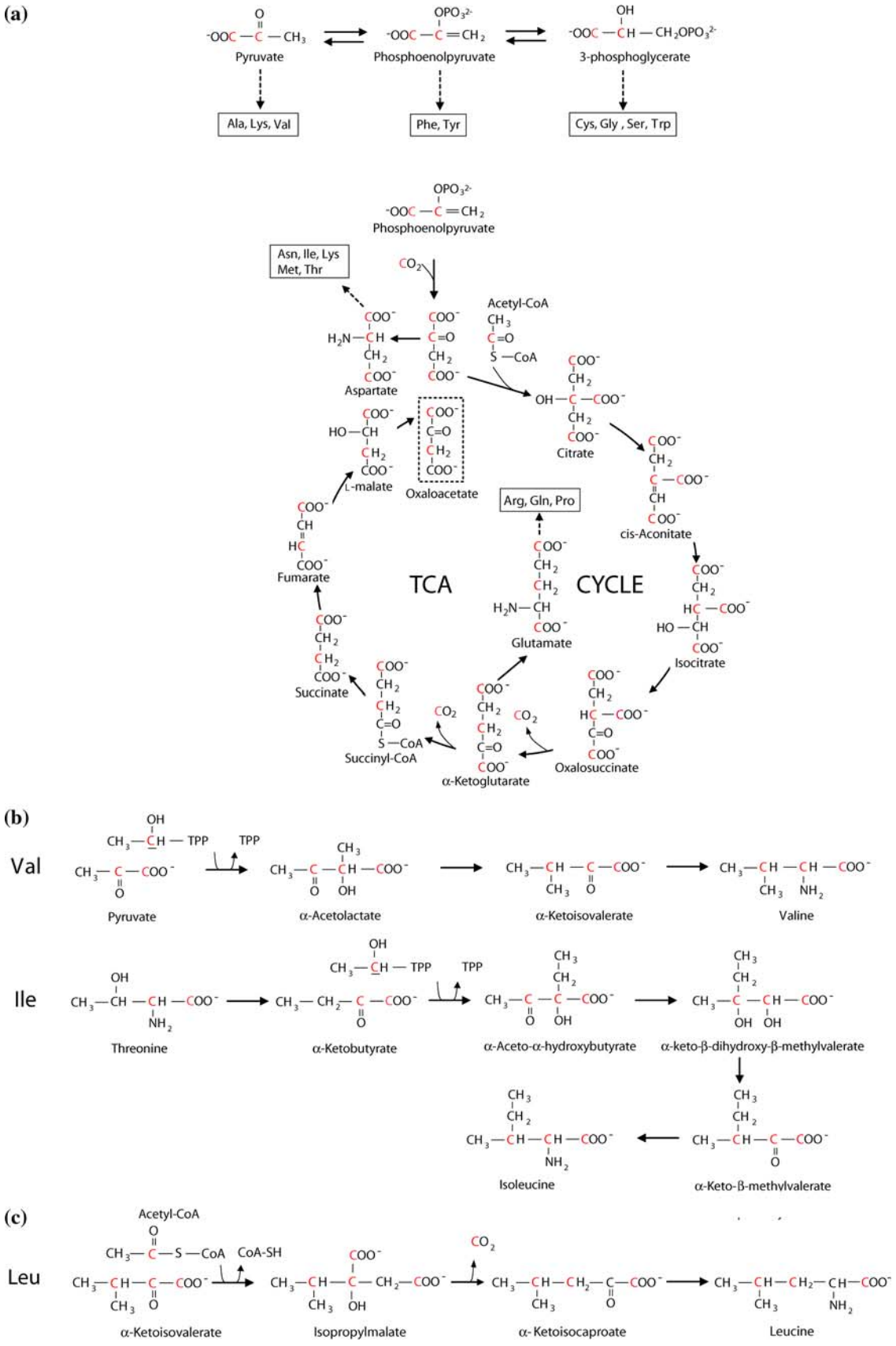
(a)
Pyruvate
Phosphoenolpyruvate
3-phosphoglycerate
Ala, Lys, Val
Phe, Tyr
Cys, Gly , Ser, Trp
Asn, Ile, Lys
Met, Thr
Aspartate
Acetyl-CoA
Citrate
L-malate
Oxaloacetate
Arg, Gln, Pro
cis-Aconitate
Fumarate
TCA CYCLE
Glutamate
Isocitrate
Succinate
Succinyl-CoA
α-Ketoglutarate
Oxalosuccinate
(b)
Val
Pyruvate
α-Acetolactate
α-Ketoisovalerate
Valine
Ile
Threonine
α-Ketobutyrate
α-Aceto-α-hydroxybutyrate
α-keto-β-dihydroxy-β-methylvalerate
Isoleucine
α-Keto-β-methylvalerate
(c)
Leu
α-Ketoisovalerate
Isopropylmalate
α-Ketoisocaproate
Leucine

◀ **Fig. 1** Major biosynthetic pathways showing the mechanisms of ^{13}C enrichment at C^{α} and CO positions of amino-acids in proteins obtained using {1,2-$^{13}C_2$}-pyruvate as the sole carbon source for **a** pyruvate- (*top row*), OA- and AKG-derived amino-acid families, **b** Val, Ile and **c** Leu. ^{13}C-enriched carbons are shown in *red*. Only the first TCA cycle is shown. The pathway for biosynthesis of His is distinct from all other amino-acids and is not shown. Lys is shown twice since it can be derived from either pyruvate or OA. The carboxylation of PEP to OA is assumed to occur with ^{13}C-enriched CO_2 to account for high levels of ^{13}CO enrichment in the AKG-derived family of amino-acids (see text)

obtain better statistics of ^{13}C incorporation levels into $^{13}C^{\alpha}$-^{13}CO spin pairs. Two samples of each protein have been obtained in D_2O-based M9 minimal media of BL21 *E. coli* cells—(1) using {1,2-$^{13}C_2$}-pyruvate as carbon source, and (2) using {U-^{13}C}-glucose as carbon source. The {1,2-$^{13}C_2$}-pyruvate-based protein production protocol closely followed the procedure described earlier (Rosen et al. 1996; Sheppard et al. 2009). We note that H_2O-based media can be used equally well for small proteins the size of GB1. The conclusions drawn here with respect to ^{13}C incorporation levels and labeling patterns are not affected to any extent by the type of the solvent chosen for protein production. The two samples of MSG were further unfolded and re-folded to completely protonate the amides buried in the hydrophobic core of the protein and exclude any possible differences in the amide D → H exchange rates between the two samples (Tugarinov et al. 2002).

Figure 2 shows the obtained ^{13}C enrichment levels in C^{α}-CO pairs of nuclei for the amino acids of groups I to III in GB1 (Fig. 2a) and MSG (Fig. 2b). ^{13}C incorporation levels have been quantified by calculating the average ratios of cross-peak intensities obtained for each amino-acid type in the pairs of identically recorded 3D HN(CO)CA-CT (constant time evolution for $^{13}C^{\alpha}$ nuclei) spectra for GB1 and 3D HN(CO)CA-TROSY spectra in the implementation of (Nietlispach 2005) for MSG acquired upon the {1,2-$^{13}C_2$}-pyruvate- and {U-^{13}C}-glucose-derived samples. The concentrations of the {1,2-$^{13}C_2$}-pyruvate- and {U-^{13}C}-glucose-derived samples have been adjusted to approximately the same values. To obtain as accurate estimates of ^{13}C incorporation into C^{α}-CO pairs as possible, the remaining (slight) differences in sample concentrations have been accounted for by normalizing by averages of peak intensities in ^{1}HN-^{15}N HSQC(^{1}HN-^{15}N TROSY) data sets of GB1(MSG), with the enrichment rate for residue i defined as $L_i = (I_{p,i}/N_p)/(I_{u,i}/N_u)$, where $I_{p,i}(I_{u,i})$ are peak intensities in the {1,2-$^{13}C_2$}-pyruvate-({U-^{13}C}-glucose-)-derived samples, N_p and N_u are normalization factors corresponding to the average peak intensities in the 2D ^{1}HN-^{15}N correlation maps of the two samples. Although glucose- and pyruvate-derived samples would have different (residual) protonation patterns, C^{α} positions of both samples are completely deuterated in D_2O-based protein production (Rosen et al. 1996). Therefore, slightly different protonation patterns/levels in the {1,2-$^{13}C_2$}-pyruvate- and {U-^{13}C}-glucose-derived samples are not expected to affect the quantified ^{13}C incorporation levels to any significant extent.

The conclusions drawn from analysis of biosynthetic pathways in Fig. 1 are largely borne out by experimental data in both proteins (Fig. 2). The C^{α}-CO pairs of amino-acids in group I are ^{13}C-enriched to more than 80%–90%(83%) on average for GB1(MSG); the enrichment levels below 100% may be due to auxiliary biosynthetic routes, such as pentose phosphate pathway that would ultimately yield unlabeled pyruvate. The levels of ^{13}C incorporation into C^{α}-CO pairs of Lys is lower, 78% (53%) on average in GB1(MSG) samples but still exceeding that of the OA-derived residues of group II, since C^{α} position of Lys can originate from either position 2 of OA or directly from position 2 of pyruvate (Fig. 1a). The enrichment of C^{α}-CO pairs in the OA-derived amino-acids (group II) is substantially lower (29 and 30% on average in GB1 and MSG, respectively) indicating that a significant flux through the TCA cycle occurs resulting in the loss of ^{13}C labels (Fig. 1a). Significant variation in ^{13}C incorporation into C^{α}-CO pairs is observed between the two proteins for a number of amino-acid types. This is especially noticeable for Ala, Lys, Gly from group I of amino-acids, and Thr, Asn from group II (compare Fig. 2a, b). The samples of both proteins have been obtained using the same cell line and the growth conditions identical in all respects except for the time the cells have been cultivated after induction of protein over-expression (8 h for MSG vs. 4.5 h in the case of GB1). It is plausible that the contribution of auxiliary biosynthetic pathways varies with the growth period after induction leading to variations in ^{13}C enrichment levels that can not be accounted for by the pathway shown in Fig. 1a. Lys represents a special case in this respect, as the relative proportion of pyruvate- and OA-derived lysine might vary depending on growth conditions.

The enrichment level of the OA-derived amino acids is a function of the rate of carboxylation of PEP (and subsequent direct incorporation of OA into amino acids of group II) relative to the flux of OA into the TCA cycle (Lundström et al. 2008). It is of interest to note that earlier reports showed the possibility of almost complete suppression of the TCA cycle during protein biosynthesis under anaerobic conditions (Szyperski 1995; Sauer et al. 1999). It remains to be seen, however, if the role of anaplerotic generation of OA under such anaerobic growth conditions can be sustained in the course of pyruvate-based protein production.

As expected, the C^{α}-CO pairs of the AKG-derived family of amino-acids (group III) are ^{13}C-enriched only at

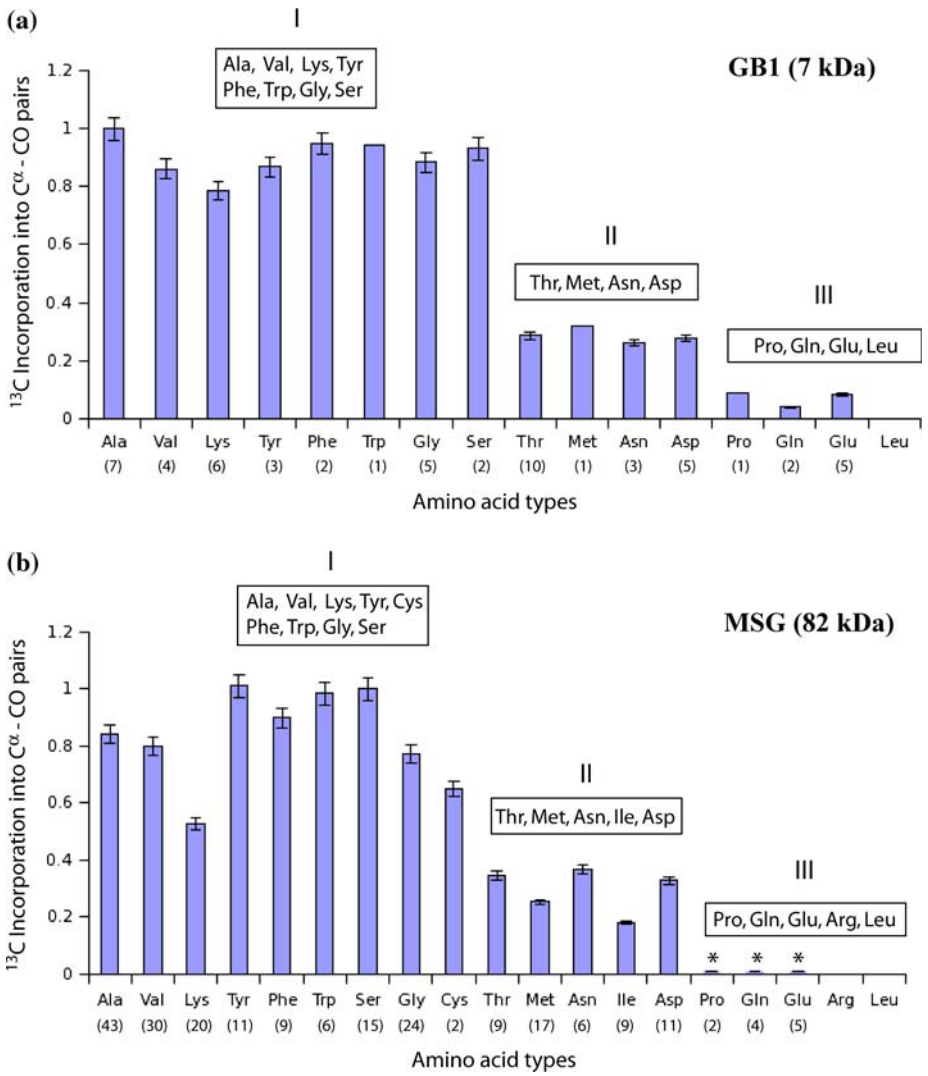

Fig. 2 ^{13}C incorporation levels in C$^{\alpha}$-CO pairs of nuclei for the amino acids of groups I through III calculated from the ratios of cross-peak intensities obtained in **a** 3D HN(CO)CA-CT experiments recorded on {1,2-$^{13}C_2$}-pyruvate-derived and {U-^{13}C}-glucose-derived GB1 (22°C; 600 MHz), and **b** 3D HN(CO)CA-TROSY experiments recorded on {1,2-$^{13}C_2$}-pyruvate-derived and {U-^{13}C}-glucose-derived MSG (37°C; 600 MHz). The ^{13}C incorporation levels are calculated based on averages over all residues of the same amino-acid type (see text). Ile, Cys, and Arg residues are missing from the sequence of GB1. Leu (no $^{13}C^{\alpha}$-^{13}CO labeling observed) has been attributed to group III. His (no $^{13}C^{\alpha}$-^{13}CO pairs observed) is omitted from the list of amino-acids. Asterisks in (**b**) mark the residues of MSG where the measurement of peak intensities was problematic due to very low signal-to-noise ratio, and the average ^{13}C incorporation level is therefore likely to be underestimated. Error bars correspond to ±r.m.s.d. values of the intensity ratios calculated for all the peaks of a given amino-acid type, while the values shown in parentheses under amino-acid three-letter codes indicate the number of peaks quantified for each amino acid type

very low levels (6% on average in GB1 and largely undetectable in MSG). Residual ^{13}C enrichment of C$^{\alpha}$-CO pairs in this family of amino-acids presumably results from auxiliary biosynthetic pathways that are not taken into account by the scheme in Fig. 1a. Of note, whenever the AKG-derived correlations were observed in the HN(CO)CA-CT spectra of the {1,2-$^{13}C_2$}-pyruvate-derived GB1 their phases indicated that C$^{\beta}$ positions are not ^{13}C-enriched (see below), contrary to predictions of Fig. 1a. No $^{13}C^{\alpha}$ (and hence no $^{13}C^{\alpha}$-^{13}CO) incorporation in Leu (Fig. 1c) could be detected in 3D HN(CO)CA data sets of either GB1 or MSG samples, although 3D HNCO(HNCO-TROSY) spectra recorded on GB1(MSG) indicated that Leu carbonyls are ^{13}C-enriched at high (>90%) levels in both proteins. His residues (missing in GB1) did not provide correlations in either the 3D HNCO-TROSY or 3D HN(CO)CA-TROSY data sets of {1,2-$^{13}C_2$}-pyruvate-derived MSG indicating that despite that its C$^{\alpha}$ position is expected to be ^{13}C-enriched in the {1,2-$^{13}C_2$}-pyruvate-derived samples, its CO positions remain ^{12}C.

From the pool of $^{13}C^{\alpha}$-^{13}CO-labeled amino-acids, only Val and Ile are ^{13}C-enriched at both C^{α} and C^{β} positions at the same time. Figure 3 shows a region of a set of superimposed 2D $F_1(^{13}C^{\alpha})$–$F_3(^{1}HN)$ planes of the HN(CO)CA-CT spectrum recorded on the {1,2-$^{13}C_2$}-pyruvate-derived sample of GB1. All the correlations originating from the amides following valine residues (there are no isoleucines in GB1) have opposite signs relative to the rest of the peaks due to evolution of $^{1}J_{C\alpha C\beta}$ scalar couplings during the constant-time period. In addition, only correlations belonging to the amides following Ile and Val residues have been observed in the 3D HN(CO)CACB-TROSY spectra recorded on the {1,2-$^{13}C_2$}-pyruvate-derived sample of MSG (data not shown) allowing us to confirm that Ile and Val are ^{13}C-enriched at both C^{α} and C^{β} sites.

The patterns of residue-specific ^{13}C labeling in C^{α}-CO pairs of nuclei is very similar to that achieved for C^{α} sites in either {2-^{13}C}-glycerol- (Takeuchi et al. 2008; LeMaster and Kushlan 1996) or {2-^{13}C}-glucose-based (Lundström et al. 2007) protein production. Whereas the ^{13}CO labeling of AKG-derived amino-acids (group III) can be 'boosted' by addition of $NaH^{13}CO_3$ to the growth medium (Lundström et al. 2008; Hansen et al. 2008), no such possibility can be envisaged for increasing the levels of ^{13}C enrichment in C^{α}-CO pairs in the present case. In fact, the same analysis

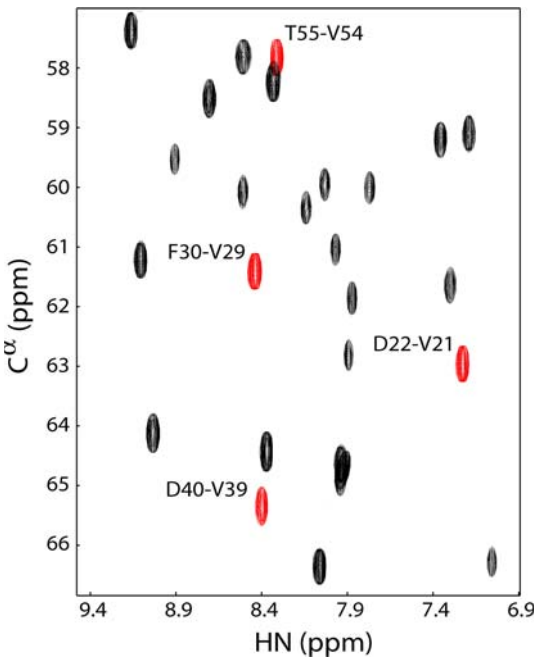

Fig. 3 A region of a set of superimposed 2D $F_1(^{13}C^{\alpha})$–$F_3(^{1}HN)$ planes of the 3D HN(CO)CA-CT experiment recorded on the sample of {1,2-$^{13}C_2$}-pyruvate-derived GB1 (22°C, 600 MHz). Negative peaks are shown with *red* contours and belong to the amide correlations following Val residues (Ile residues are absent from the sequence of GB1). Each negative correlation is labeled with the number and type of [residue *i*–residue *i*−1] pair, where residue *i*-1 is valine

as described above applied to 3D HNCO(HNCO-TROSY) spectra recorded on GB1(MSG) shows that the levels of ^{13}C incorporation into carbonyl positions of group III amino-acids in this work are substantially higher (74 and 72% in GB1 and MSG, respectively) than those reported by (Lundström et al. 2008) for the case of {1-^{13}C}-pyruvate-derived proteins (~26% for groups II and III on average). Although analysis of subsequent TCA cycles (following the first one shown in Fig. 1a) indicates that ^{13}CO labeling of group III amino-acids would occur with 50% probability after the second and third TCA cycles in {1,2-$^{13}C_2$}-pyruvate-based protein growths *even if* PEP is carboxylated with *unlabeled* CO_2, the experimentally observed high levels of ^{13}CO enrichment in the AKG family can not be even qualitatively explained by this observation implying that the carboxylation of PEP to OA in the {1,2-$^{13}C_2$}-pyruvate-based protein production occurs already with predominantly ^{13}C-enriched CO_2 in the absence of $NaH^{13}CO_3$ in the medium (see Fig. 1a). Indeed, it can be expected that a larger fraction of the metabolic CO_2 will be ^{13}C-labeled if {1,2-$^{13}C_2$}-pyruvate is used instead of {1-^{13}C}-pyruvate as carbon source. Finally, based on analysis of biosynthetic pathways in Fig. 1a and experimental data, we note that {1,2-$^{13}C_2$}-pyruvate-based protein production generates (at least partially) ^{13}C-enriched C^{β} positions in the side-chains of Val, Ile (as described above), His, Leu and all amino-acids of group III; ^{13}C-enriched C^{γ} positions in the side-chains of the OA-derived amino-acids (group II, including $C^{\gamma 2}$ methyl position of Thr) as well as in Tyr, Phe, and Leu; and ^{13}C-enriched C^{δ} positions in amino-acids of group III.

In summary, we have described a labeling approach for producing proteins with selectively ^{13}C-enriched backbone nuclei ($^{13}C^{\alpha}$-^{13}CO pairs) in 12 out of 20 amino-acid types. High labeling efficiency is obtained in isolated $^{13}C^{\alpha}$-^{13}CO pairs of Ala, Cys, Gly, Ser, Trp, Phe, Tyr, and Lys amino-acids; lower enrichment levels (~20–40%) are obtained in Asn, Asp, Met, and Thr. None or very low incorporation levels are observed in $^{13}C^{\alpha}$-^{13}CO pairs of His, Leu, Arg, Pro, Glu, and Gln, while only in Val and Ile C^{β} sites are ^{13}C-enriched along with $^{13}C^{\alpha}$-^{13}CO labeling. A number of NMR applications may benefit from the described labeling scheme. Direct ^{13}C detection techniques (Bermel et al. 2005a, b; Lee et al. 2005; Serber et al. 2001; Takeuchi et al. 2008) can be applied to deuterated {1,2-$^{13}C_2$}-pyruvate-derived protein samples provided that efficient 'homo-decoupling' methods are employed. Although {1,2-$^{13}C_2$}-pyruvate is available commercially, it is at least as expensive as {U-^{13}C,^{2}H}-labeled glucose. Because of the costs involved in {1,2-$^{13}C_2$}-pyruvate-based protein production and because a significant portion of residues remains unlabeled in C^{α}-CO pairs, we do not anticipate that the described labeling scheme would become a part of a viable strategy for ^{13}C detection-based sequential resonance

assignments in proteins. Instead, it is more likely to be of use for more specialized applications. For example, it can be envisaged that relaxation properties of deuterated $^{13}C^{\alpha}$ positions in proteins can be studied via triple-resonance techniques in the subset of selectively $^{13}C^{\alpha}$-^{13}CO-labeled residues provided that $^{13}C^{\alpha}$-^{13}CO dipolar interactions are taken into account. The elimination of $^{13}C^{\alpha}$-$^{13}C^{\beta}$ J couplings in 12 amino-acid types would allow the recording of such triple-resonance-type spectra with higher resolution in the carbon dimension. In addition, in large and complex protein structures where assignment of resonances is an issue, the selectivity of {1,2-$^{13}C_2$}-pyruvate-based labeling with respect to incorporation levels in different amino-acids, can be of help for independent verification of backbone resonance assignments (Tugarinov et al. 2002).

Acknowledgments This work was supported in part by the Nano-Biotechnology Award to VT (University of Maryland). The authors are grateful to Dr. Patrik Lundström (University of Toronto) for helpful discussions related to pyruvate-based isotope labeling of proteins.

References

Bermel W, Bertini I, Duma L, Felli IC, Emsley L, Pieratelli R, Vasos PR (2005a) Complete assignment of heteronuclear protein resonances by protonless NMR spectroscopy. Angew Chem Int Ed 44:3089–3092

Bermel W, Bertini I, Felli IC, Pieratelli R, Vasos PR (2005b) A selective experiment for the sequential protein backbone assignment from 3D heteronuclear spectra. J Magn Reson 172:324–328

Gardner KH, Kay LE (1998) The use of ^{2}H, ^{13}C, ^{15}N multidimensional NMR to study the structure and dynamics of proteins. Annu Rev Biophys Biomol Struct 27:357–406

Gardner KH, Rosen MK, Kay LE (1997) Global folds of highly deuterated, methyl protonated proteins by multidimensional NMR. Biochemistry 36:1389–1401

Goto NK, Kay LE (2000) New developments in isotope labeling strategies for protein solution NMR spectroscopy. Curr Opin Struct Biol 10:585–592

Hansen DF, Vallurupalli P, Lundström P, Neudecker P, Kay LE (2008) Probing chemical shifts of invisible states of proteins with relaxation dispersion NMR spectroscopy: how well can we do? J Am Chem Soc 130:2667–2675

Ishima R, Louis JM, Torchia DA (2001) Optimized labeling of $^{13}CHD_2$—methyl isotopomers in perdeuterated proteins: potential advantages for ^{13}C relaxation studies of methyl dynamics in larger proteins. J Biomol NMR 21:167–171

Kainosho M (1997) Isotope labeling of macromolecules for structural determinations. Nat Struct Biol 4:858–861

Kainosho M, Torizawa T, Iwashita Y, Terauchi T, Mei Ono A, Guntert P (2006) Optimal isotope labeling for NMR protein structure determinations. Nature 440:52–57

Lee AL, Urbauer JL, Wand AJ (1997) Improved labeling strategy for ^{13}C relaxation measurements of methyl groups in proteins. J Biomol NMR 9:437–440

Lee D, Vogeli B, Pervushin K (2005) Detection of C′, C^{α} correlations in proteins using a new time- and sensitivity-optimal experiment. J Biomol NMR 31:273–278

LeMaster DM, Kushlan DM (1996) Dynamical mapping of *E. coli* thioredoxin via ^{13}C NMR relaxation analysis. J Am Chem Soc 118:9255–9264

Lian LY, Middleton DA (2001) Labelling approaches for protein structural studies by solution-state and solid-state NMR. Prog Nucl Magn Reson Spectrosc 39:171–190

Lundström P, Teilum K, Carstensen T, Bezsonova I, Wiesner S, Hansen DF, Religa TL, Akke M, Kay LE (2007) Fractional ^{13}C enrichment of isolated carbons using [1-^{13}C]- or [2-^{13}C]-glucose facilitates the accurate measurement of dynamics at backbone C^{α} and side-chain methyl positions in proteins. J Biomol NMR 38:199–212

Lundström P, Hansen DF, Kay LE (2008) Measurement of carbonyl chemical shifts of excited protein states by relaxation dispersion NMR spectroscopy: comparison between uniformly and selectively ^{13}C-labeled samples. J Biomol NMR 42:35–47

Nietlispach D (2005) Suppression of anti-TROSY lines in a sensitivity enhanced gradient selection TROSY scheme. J Biomol NMR 31:161–166

Rosen MK, Gardner KH, Willis RC, Parris WE, Pawson T, Kay LE (1996) Selective methyl group protonation of perdeuterated proteins. J Mol Biol 263:627–636

Sauer U, Lasko DR, Fiaux J, Hochuli M, Glaser R, Szyperski T, Wüthrich K, Bailey JE (1999) Metabolic flux ratio analysis of genetic and environmental modulations of *E. coli* central carbon metabolism. J Bacteriol 181:6679–6688

Serber Z, Richter C, Dötsch V (2001) Carbon-detected NMR experiments to investigate structure and dynamics of biological macromolecules. Chembiochem 2:247–251

Sheppard D, Guo C, Tugarinov V (2009) Methyl-detected 'out-and-back' NMR experiments for simultaneous assignments of Alaβ and Ileγ2 methyl groups in large proteins. J Biomol NMR 43:229–238

Szyperski T (1995) Biosynthetically directed fractional ^{13}C-labeling of proteinogenic amino acids. An efficient analytical tool to investigate intermediary metabolism. Eur J Biochem 232:433–448

Takeuchi K, Ng E, Malia TJ, Wagner G (2007) 1–^{13}C amino acid selective labeling in a $^{2}H^{15}N$ background for NMR studies of large proteins. J Biomol NMR 38:89–98

Takeuchi K, Sun ZYJ, Wagner G (2008) Alternate ^{13}C–^{12}C labeling for complete main chain resonance assignments using C^{α} direct-detection with applicability toward fast relaxing protein systems. J Am Chem Soc 130:17210–17211

Teilum K, Brath U, Lundström P, Akke M (2006) Biosynthetic ^{13}C labeling of aromatic side chains in proteins for NMR relaxation measurements. J Am Chem Soc 128:2506–2507

Tugarinov V, Muhandiram R, Ayed A, Kay LE (2002) Four-dimensional NMR spectroscopy of a 723-residue protein: chemical shift assignments and secondary structure of malate synthase G. J Am Chem Soc 124:10025–10035

Tugarinov V, Hwang PM, Kay LE (2004) Nuclear magnetic resonance spectroscopy of high-molecular-weight proteins. Annu Rev Biochem 73:107–146

Tugarinov V, Kanelis V, Kay LE (2006) Isotope labeling strategies for the study of high-molecular-weight proteins by solution NMR spectroscopy. Nat Protoc 1:749–754